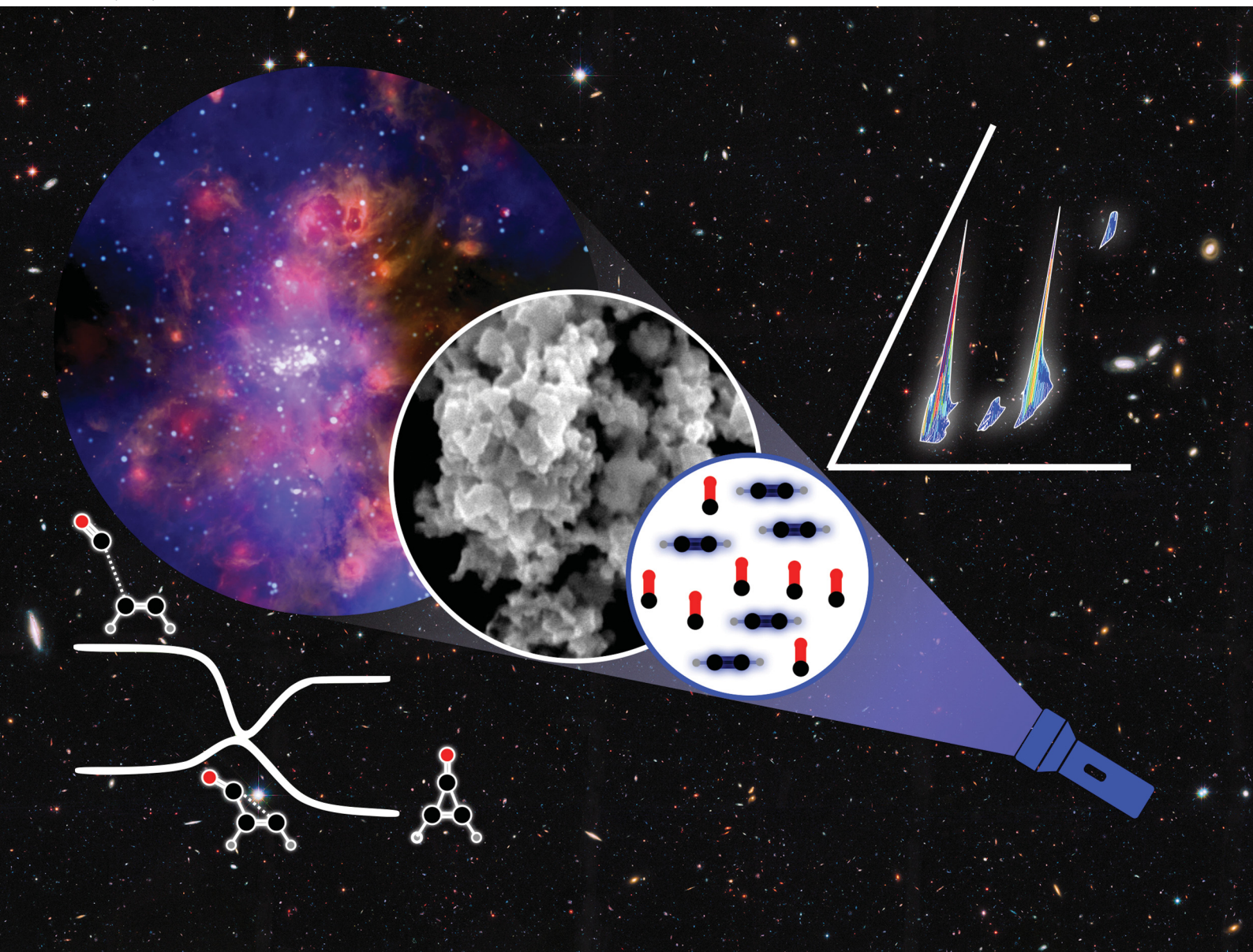


PCCP

Physical Chemistry Chemical Physics

rsc.li/pccp



ISSN 1463-9076

PAPER

Samer Gozem, Ralf I. Kaiser *et al.*
Photochemically triggered cheletropic formation of
cyclopropanone ($c\text{-C}_3\text{H}_2\text{O}$) from carbon monoxide and
electronically excited acetylene


 Cite this: *Phys. Chem. Chem. Phys.*,
 2022, 24, 17449

Photochemically triggered cheletropic formation of cyclopropenone (c-C₃H₂O) from carbon monoxide and electronically excited acetylene†

 Jia Wang,^{ab} N. Fabian Kleimeier,^{ab} Rebecca N. Johnson,^c Samer Gozem,^{id *c}
 Matthew J. Abplanalp,^{ab} Andrew M. Turner,^{ab} Joshua H. Marks^{ab} and
 Ralf I. Kaiser^{id *ab}

For more than half a century, pericyclic reactions have played an important role in advancing our fundamental understanding of cycloadditions, sigmatropic shifts, group transfer reactions, and electrocyclization reactions. However, the fundamental mechanisms of photochemically activated cheletropic reactions have remained contentious. Here we report on the simplest cheletropic reaction: the [2+1] addition of ground state ¹⁸O-carbon monoxide (C¹⁸O, X¹Σ⁺) to D₂-acetylene (C₂D₂) photochemically excited to the first excited triplet (T₁), second excited triplet (T₂), and first excited singlet state (S₁) at 5 K, leading to the formation of D₂-¹⁸O-cyclopropenone (c-C₃D₂¹⁸O). Supported by quantum-chemical calculations, our investigation provides persuasive testimony on stepwise cheletropic reaction pathways to cyclopropenone via excited state dynamics involving the T₂ (non-adiabatic) and S₁ state (adiabatic) of acetylene at 5 K, while the T₁ state energetically favors an intermediate structure that directly dissociates after relaxing to the ground state. The agreement between experiments in low temperature ices and the excited state calculations signifies how photolysis experiments coupled with theoretical calculations can untangle polyatomic reactions with relevance to fundamental physical organic chemistry at the molecular level, thus affording a versatile strategy to unravel exotic non-equilibrium chemistries in cyclic, aromatic organics. Distinct from traditional radical–radical pathways leading to organic molecules on ice-coated interstellar nanoparticles (interstellar grains) in cold molecular clouds and star-forming regions, the photolytic formation of cyclopropenone as presented changes the perception of how we explain the formation of complex organics in the interstellar medium eventually leading to the molecular precursors of biorelevant molecules.

 Received 30th April 2022,
 Accepted 8th June 2022

DOI: 10.1039/d2cp01978g

rsc.li/pccp

1. Introduction

For more than half a century, pericyclic reactions—reactions that proceed *via* a single, concerted transition state allowing a cyclic overlap of π and/or σ orbitals—have played a central role in advancing our fundamental understanding of cycloadditions,¹ sigmatropic shifts,² group transfer reactions,² electrocyclization,³ and cheletropic reactions.^{4,5} The mechanistical understanding

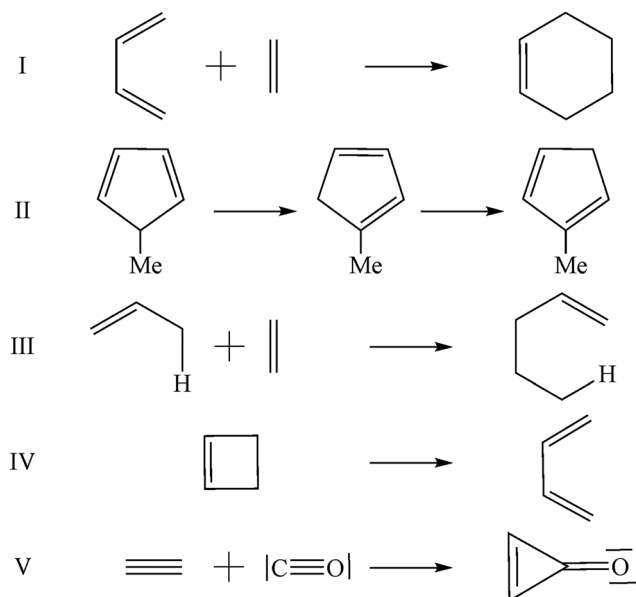
of pericyclic reactions has impacted electronic structure and chemical bonding theory² as well as preparative organic chemistry on the industrial scale (Scheme 1).^{6,7} Early formulations of the pericyclic selection rules evolved from Frontier Molecular Orbital (FMO) theory,⁸ where a pericyclic reaction is coined symmetry-forbidden or symmetry-allowed to indicate existence or absence of a symmetry-imposed barrier, respectively.⁹ These symmetry considerations are derived from a correlation diagram connecting the ground and excited electronic states of the reactants and products. For instance, symmetry-forbidden reactions proceed with barriers reaching up to 500 kJ mol⁻¹ for thermal [2+2] cycloadditions of two ethylene (C₂H₄) molecules to cyclobutadiene (C₄H₈).^{10,11} Cheletropic reactions, where one reactant forms both bonds from the same atom with a co-reactant (Scheme 2), are pericyclic reactions that have received much attention for their utility in preparing cyclic molecules from acyclic precursors.^{12,13} The symmetry allowed [2+1] additions of electronically excited singlet carbene (CH₂, a¹A₁) to the π-electronic system of ethylene (C₂H₄) and acetylene

^a Department of Chemistry, University of Hawaii at Manoa, Honolulu, HI 96822, USA. E-mail: ralfk@hawaii.edu

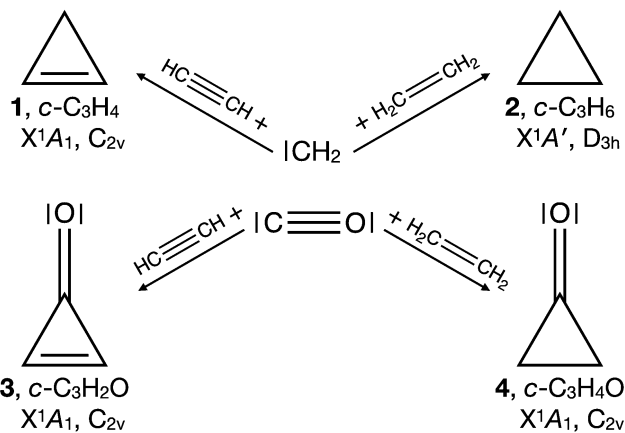
^b W. M. Keck Research Laboratory in Astrochemistry, University of Hawaii at Manoa, Honolulu, HI 96822, USA

^c Department of Chemistry, Georgia State University, Atlanta, GA 30302, USA. E-mail: sgozem@gsu.edu

† Electronic supplementary information (ESI) available: Experimental details, quantum chemical calculations, Table S1, Fig. S1–S4, Cartesian coordinates of key structures, and absolute energies. See DOI: <https://doi.org/10.1039/d2cp01978g>



Scheme 1 Examples of pericyclic reactions: cycloaddition (I), sigmatropic shift (II), group transfer reaction (III), electrocyclization (IV), and cheletropic reaction (V).



Scheme 2 Schematic representation of cheletropic reactions of singlet carbene (CH_2) with acetylene (C_2H_2) and ethylene (C_2H_4) leading to cyclopropene (C_3H_4 , **1**) and cyclopropane (C_3H_6 , **2**) and of carbon monoxide (CO) with acetylene (C_2H_2) and ethylene (C_2H_4) forming cyclopropenone ($\text{c-C}_3\text{H}_2\text{O}$, **3**) and cyclopropanone ($\text{c-C}_3\text{H}_4\text{O}$, **4**), respectively.

(C_2H_2), leading to cyclopropane (C_3H_6) and cyclopropene (C_3H_4), respectively, are among the most influential cycloadditions from the fundamental and synthetic point of view.^{14–18} Cheletropic reactions have been exploited in preparative organic chemistry to synthesize, *e.g.*, annulenes and prodrugs *via* carbon monoxide (CO) elimination,¹⁹ chiral phosphonium cations,²⁰ enantiomerically-pure carbocycles,²¹ and exotic enedynes.²²

Despite their importance, there is still an incomplete understanding of the fundamental mechanisms of photochemically activated cheletropic reactions. Debated mechanistic aspects are linear *versus* non-linear approach geometry of reactants,^{23,24}

a Hückel *versus* Möbius (anti) aromatic character of the π -system,²⁵ the excited state surfaces and crossings involved,²⁶ and concerted *versus* stepwise mechanisms.²⁷ An disentangling of these key questions requires an experimental investigation of cheletropic reactions involving simple, prototype systems, which can be benchmarked and compared to computational studies. The insights derived from such ‘simple’ benchmarks are critical not only to understand the reactivity of cheletropic reactions on a molecular level, but can also indicate how to control the outcome of (stereospecific) reaction pathways in more complex systems of practical importance, *e.g.*, for synthetic chemistry, drug design, and astrochemistry.

Here, we report on the simplest excited-state cheletropic reaction: the [2+1] photochemical addition of ground state ^{18}O -carbon monoxide (C^{18}O , $\text{X}^1\Sigma^+$) to electronically excited D2-acetylene (C_2D_2) leading to the formation of D2- ^{18}O -cyclopropenone ($\text{c-C}_3\text{D}_2^{18}\text{O}$, **3**; eqn (1)).



Specifically, we investigate D2-acetylene excited to the first excited triplet (T_1), second excited triplet (T_2), and first excited singlet state (S_1) by 222 nm (5.58 eV), 249 nm (4.98 eV), and 288 nm (4.31 eV), respectively (Fig. 1). Experiments are carried out at low temperature ices at 5 K. The photon energies employed are below the first excited electronic state of carbon monoxide (6.010 ± 0.04 eV),²⁸ the carbon–deuterium bond energy (5.797 ± 0.006 eV),²⁹ and the adiabatic ionization energies of carbon monoxide (14.0142 ± 0.0003 eV)³⁰ and D2-acetylene (11.416 ± 0.006 eV).³¹ Therefore, the photon energies used exclude ion–molecule reactions and simple carbon–deuterium bond rupture processes. These wavelengths were chosen to explore the effect of distinct low-lying electronically excited states on the low-temperature reactivity of D2-acetylene and how they influence the cheletropic character of the reaction. These surface-science experiments are merged with multi-reference *ab initio* calculations exploring the formation mechanism of D2- ^{18}O -cyclopropenone ($\text{c-C}_3\text{D}_2^{18}\text{O}$, **3**). In addition to insight into mechanistic physical organic (photo)chemistry, an understanding of cheletropic reactions in the carbon monoxide–acetylene system is also of fundamental importance to accessing the scantily explored class of aromatic cyclic ketones (Scheme 3) with cyclopropenone ($\text{c-C}_3\text{H}_2\text{O}$, **3**) being their simplest representative. Along with its larger members cyclopentadienone ($\text{c-C}_5\text{H}_4\text{O}$, **5**) and cycloheptatrienone ($\text{c-C}_7\text{H}_6\text{O}$, **6**), cyclic π -conjugated ketones have attracted considerable attention due to their potential Hückel (anti)-aromaticity,^{32–39} shedding light on the electronic structure and dimerization reactions of cyclic aromatic ketones.^{38,40} The 2π and 6π aromaticity of cyclopropenone (**3**) and cyclopentadienone (**5**), respectively,⁴¹ is reflected in the dipolar resonance structures of the carbonyl double bond ($\text{C}=\text{O} \leftrightarrow \text{}^+\text{C}-\text{O}^-$) (Scheme 3)³⁸ formally leading to a carbocation with a vacant p-orbital able to foster a ring current within the delocalized 2π aromatic system.⁴²

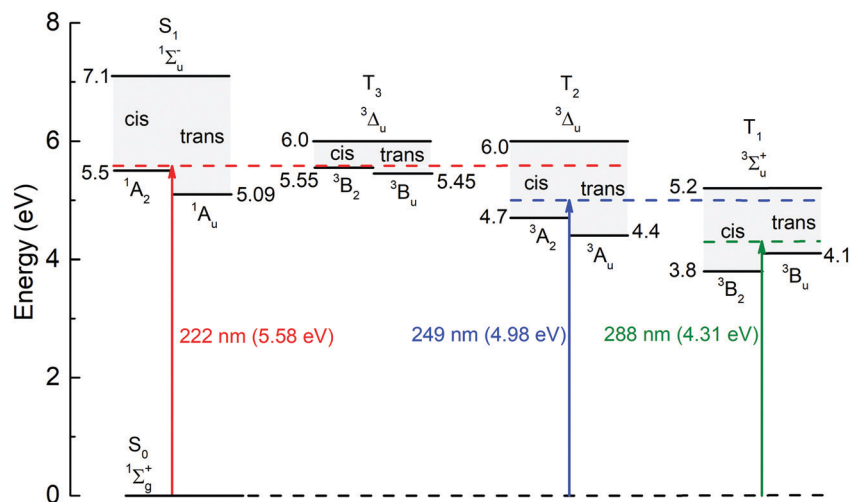
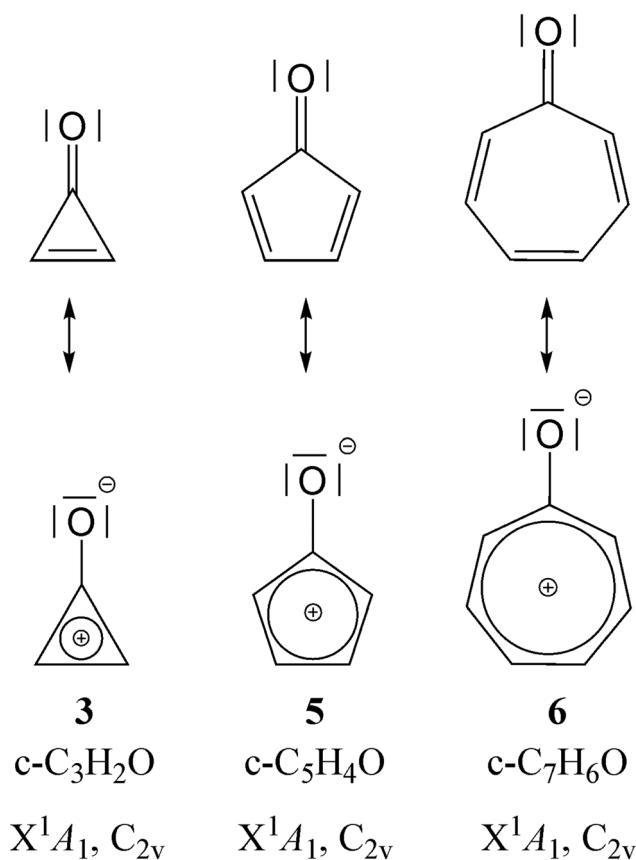


Fig. 1 Energy level diagram of the four lowest energy excited states of acetylene (T_1 , T_2 , T_3 , and S_1).⁵² The upper and lower energy limits of each state correspond to the linear symmetry (vertical excitation) and the adiabatic transitions to the *cis* and *trans* geometries, respectively. Arrows and dashed lines represent the excitation energies used in the experiments.



Scheme 3 Electronic wave functions and point groups of cycloprope-none (**3**), cyclopentadienone (**5**), and cycloheptatrienone (**6**) along with their resonance structures.

2. Results

2.1 Infrared spectroscopy

The experiments were carried out in an ultrahigh vacuum (UHV) surface-science chamber operated at pressures of a few

10^{-11} torr by photolyzing binary ices of ^{18}O -carbon monoxide (C^{18}O) and D_2 -acetylene (C_2D_2) at photon energies of 222 nm (5.58 eV), 249 nm (4.98 eV), and 288 nm (4.31 eV) at 5 K. Infrared spectroscopy signifies an important analytical tool to identify functional groups emerging during the photoactivation (Fig. S1 and Table S1, ESI[†]). Infrared spectra of the pristine $\text{C}^{18}\text{O}\text{-C}_2\text{D}_2$ ices at 5 K revealed prominent absorptions of D_2 -acetylene and ^{18}O -carbon monoxide such as the CD stretching modes (ν_1 , 2680 cm^{-1} ; ν_3 , 2408 cm^{-1}),⁴³ the C^{18}O stretching mode (ν_1 , 2088 cm^{-1}),⁴⁴ the combination modes for C_2D_2 ($\nu_1 + \nu_3$, 5042 cm^{-1} ; $\nu_1 + \nu_5$, 3294 cm^{-1} ; $\nu_3 + \nu_4$, 2929 cm^{-1} ; $\nu_2 + \nu_5$, 2327 cm^{-1} ; $\nu_4 + \nu_5$, 1077 cm^{-1}),⁴³ and the overtone of the stretching mode of C^{18}O ($2\nu_1$, 4150 cm^{-1}).⁴⁵ At 222 nm, the photoactivation resulted in a slight decrease of $4.1 \pm 3.3\%$ and $1.3 \pm 0.8\%$ of the C_2D_2 and C^{18}O reactants monitored through their stretching mode at 2408 cm^{-1} (ν_3) and 2088 cm^{-1} (ν_1), respectively (Appendix, Fig. S1, ESI[†]). Simultaneously, new absorptions emerged at 1734 cm^{-1} , 1772 cm^{-1} and 2573 cm^{-1} with the 1734 cm^{-1} feature possibly linked to the carbonyl ($\text{C}=\text{O}$) functional group of D_2 -cycloprope-none (ν_2 of $c\text{-C}_3\text{D}_2^{18}\text{O}$). The remaining absorptions can be associated with carbonyl ($\text{C}=\text{O}$) and acetylenic C-D ($-\text{C}\equiv\text{C}-\text{D}$) functional groups.^{14,38} However, due to the strong overlap of functional groups of the photoactivated mixture of organic molecules (carbonyl moieties in particular),^{45–47} infrared spectroscopy cannot unequivocally identify the products after photoexcitation.⁴⁶ Therefore, an alternative, isomer-selective technique is needed.

2.2 PI-ReTOF-MS

Photoionization reflectron time-of-flight mass spectrometry (PI-ReTOF-MS) was exploited to identify the subliming molecules isomer-specifically during temperature programmed desorption (TPD) of the photoactivated ices from 5 to 300 K.^{48,49} This technique has the exceptional advantage to distinguish structural isomers based on their distinct adiabatic ionization

energies (IEs) by systematically tuning the photon energy (PE) above and below the IE of the isomer of interest. As shown in Fig. S2 (ESI[†]), The IEs of propynal (HCOCCH, **7**), cyclopropenone (c-C₃H₂O, **3**), and propadienone (H₂CCCO, **8**) are 10.52–10.62 eV,⁵⁰ 9.22–9.32 eV,³³ and 9.04–9.14 eV,⁵¹ respectively, corrected for the Stark effect by the electric field of the ReTOF-MS optics.⁵² Therefore, two photon energies of 10.49 eV and 9.20 eV are required to detect cyclopropenone. Note that the ionization energies of the isotopically labelled (¹⁸O, D) products differ by at most 0.01 eV from the non-substituted counterparts (**3**, **7**, **8**); this is within the experimental error limits.⁵² At 10.49 eV, only cyclopropenone (**3**), and propadienone (**8**) can be ionized; the IE of propynal (**7**) is higher. Lowering the PE to 9.20 eV would only allow – if present – ionization of propadienone (**8**). Therefore, through a comparison of the TPD profiles of the C₃D₂¹⁸O ions at *m/z* = 58 at distinct PEs of 10.49 eV and 9.20 eV, the formation of **3** versus **8** can be explored at distinct photoactivation wavelengths. Fig. 2 compiles the PI-ReTOF-MS data of the molecules desorbing from the C¹⁸O–C₂D₂ ices photoactivated at 222 nm, 249 nm, and 288 nm; Fig. 3 displays the extracted TPD profiles of *m/z* = 58 (C₃D₂¹⁸O⁺) as a function of temperature at distinct photoactivation wavelengths and PEs (10.49 eV, 9.20 eV). Upon photoionization at 10.49 eV, a single sublimation event is evident from 150 K to 230 K for *m/z* = 58 of the subliming ices photoactivated at 222 nm (Fig. 3a). Recall that at PE = 10.49 eV, only **3** and **8** can be ionized. This sublimation event disappears when the PE is lowered to 9.20 eV (Fig. 3b), which would only ionize **8** (Fig. 3b). The blank experiment (Fig. 3d) was conducted under identical conditions at PE = 10.49 eV, but without photoactivation of the ices. Therefore, we conclude that at 222 nm cyclopropenone (c-C₃D₂¹⁸O, **3**) is formed. It should be stressed that the corresponding blank experiment (Fig. 3d) shows no ion counts at all; hence ions at *m/z* = 58 are the result of the photoactivation of the ices at 222 nm, but they do not originate from ion–molecule reactions in the gas phase. The sublimation range of cyclopropenone (c-C₃D₂¹⁸O, **3**) of 150–230 K agrees exceptionally well with the sublimation temperatures of cyclopropenone **3** prepared through the exposure of acetylene–carbon monoxide ices to energetic electrons at cryogenic temperatures (Fig. 3a), while the propynal isomer **7** sublimes earlier from 128–155 K.^{52,53} Separate sets of experiments were conducted to photoactivate the C¹⁸O–C₂D₂ ices at 222 nm over 0 (blank), 1, 2, 5, and 10 hours with the irradiation time plotted versus the integrated ion counts at *m/z* = 58 (Fig. 4). This graph reveals a linear dependence of the cyclopropenone yield versus time, indicating that a single photon process is involved in the formation of c-C₃D₂¹⁸O with overall yields of $7.5 \pm 1.0 \times 10^{-19}$ ion counts per photon at 222 nm. Increasing the wavelength from 222 nm to 249 nm and photoionizing the subliming molecules at 10.49 eV also depicts a TPD profile from 150–230 K at *m/z* = 58 for cyclopropenone, albeit at lower count rates despite an increase in photon flux by a factor of three (Fig. 3c). Compared to 222 nm, the ion yield is reduced to $9.7 \pm 1.3 \times 10^{-20}$ ion counts per photon at 249 nm. Increasing the wavelength further to 288 nm does not result in any ion counts above noise level despite an enhancement of the flux by a

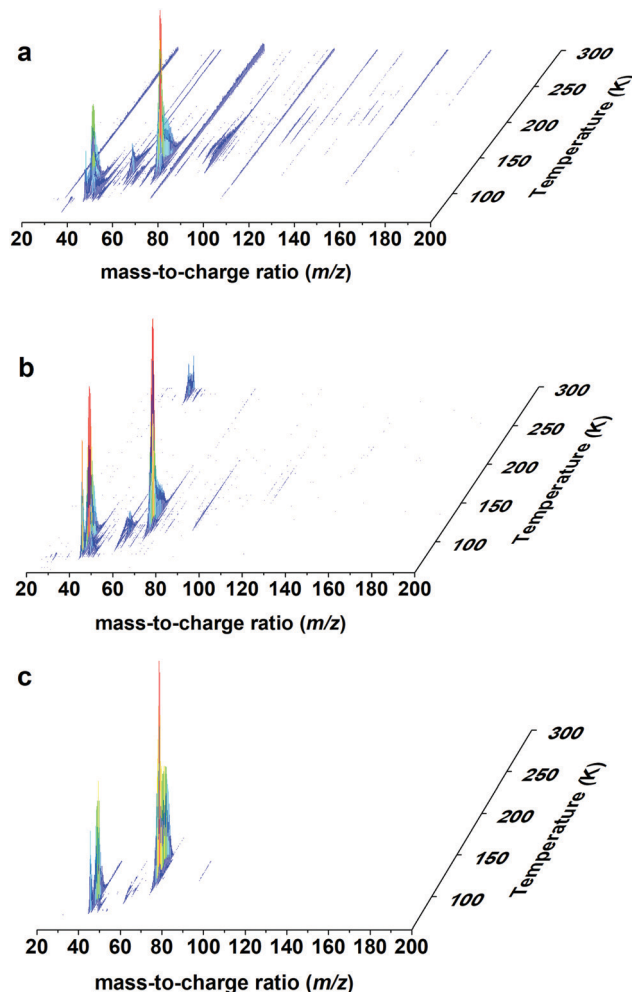


Fig. 2 PI-ReTOF-MS data displaying ion counts as a function of the temperature of the subliming molecules recorded at 10.49 eV for ¹⁸O–carbon monoxide–D₂–acetylene ices (C¹⁸O–C₂D₂) photolyzed at 222 nm (a), 249 nm (b), and 288 nm (c).

factor of four. Therefore, we find that, within our signal-to-noise limits, cyclopropenone is not formed upon photoactivation of C¹⁸O–C₂D₂ ices at 288 nm. Based on the integrated ion counts and the photoionization cross sections,⁵² formation rates of cyclopropenone are determined to be $6.9 \pm 1.1 \times 10^{-2}$ and $8.9 \pm 1.4 \times 10^{-3}$ molecules per photon for 222 nm and 249 nm, respectively (ESI[†]).

2.3 Electronic structure calculations

The PI-ReTOF-MS experiments indicate that cyclopropenone is formed photochemically after C¹⁸O–C₂D₂ ices are exposed to photons having a wavelength below 249 nm. We employ quantum chemical calculations to investigate the formation mechanism of c-C₃D₂¹⁸O starting from different low-lying excited states of C₂D₂. The calculations are performed for a gas phase model of carbon monoxide and acetylene so that multi-reference *ab initio* electronic structure methods can be used to determine ground and excited-state energetics of the cyclopropenone formation reaction. Details of the computations

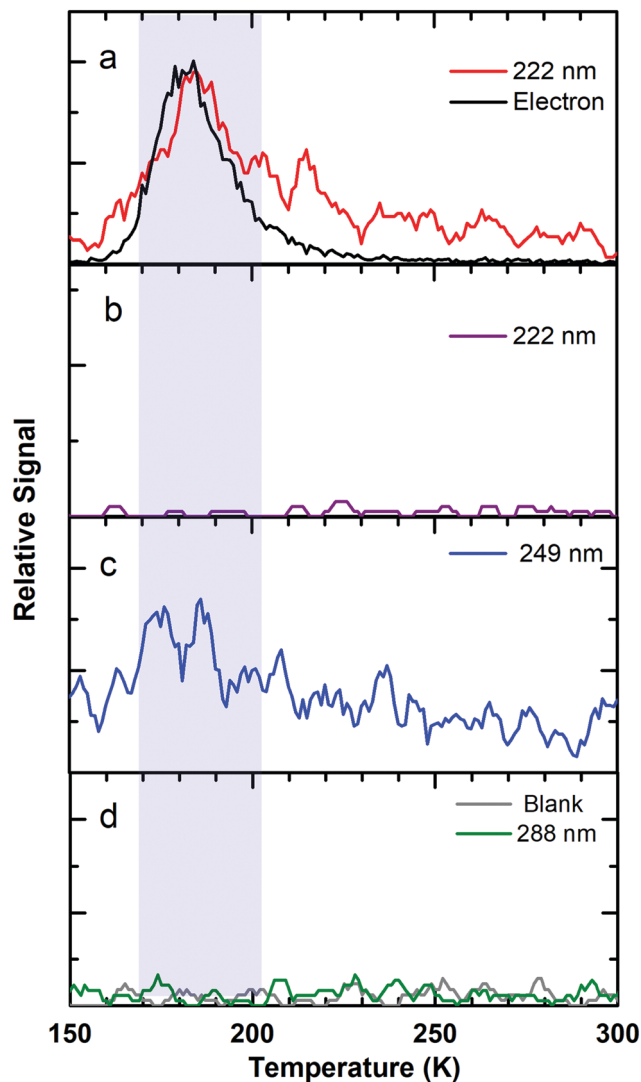


Fig. 3 TPD profiles for $m/z = 58$ ($\text{C}_3\text{D}_2^{18}\text{O}^+$) of photolyzed ices recorded at photoionization energies of 10.49 eV (a, c and d) and 9.20 eV (b). The $\text{C}^{18}\text{O}-\text{C}_2\text{D}_2$ ices were photolyzed by 222 nm (purple and red) for 10 hours, by 249 nm (blue) for 30 hours, and by 288 nm (green) for 42 hours. The blank experiment (grey) was carried out under identical conditions, but without photolysis of the ices.

are included in Section 4.2 and in the ESI.† Briefly, the complete active space (CASSCF) approach⁵⁴ and second-order perturbation energy corrections (CASPT2//CASSCF)⁵⁵ with the ANO-L-VDZP basis set^{56,57} are employed for most calculations in this work. The formation mechanism of cyclopropanone was first investigated by performing relaxed potential energy scans along a decreasing distance between the carbon atom of carbon monoxide and the acetylenic carbon atom. On the ground state potential energy surface, calculations indicate an entrance barrier of 65 kJ mol^{-1} ; *i.e.*, the barrier for formation of $c\text{-C}_3\text{H}_2\text{O}$ from the reactants $\text{CO}(\text{X}^1\Sigma^+)$ and $\text{C}_2\text{H}_2(\text{X}^1\Sigma_g^+)$. This is consistent with the fact that no $c\text{-C}_3\text{D}_2^{18}\text{O}$ was observed after heating carbon monoxide–acetylene ices from 5 K to 300 K in the “blank” experiment.

Next, the reaction between excited states of acetylene with ground state carbon monoxide are considered. For the

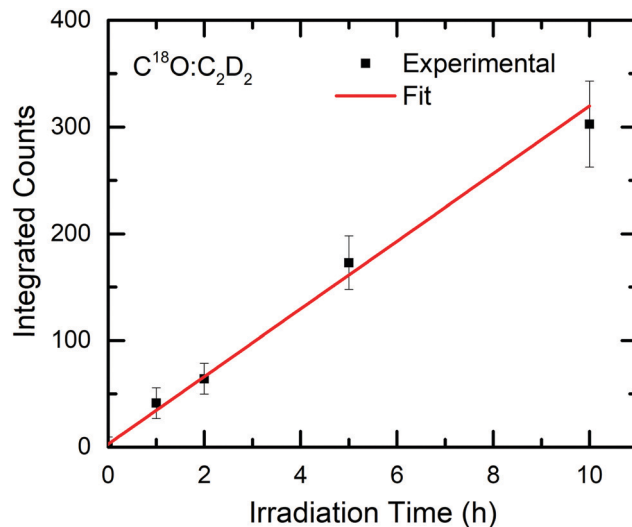
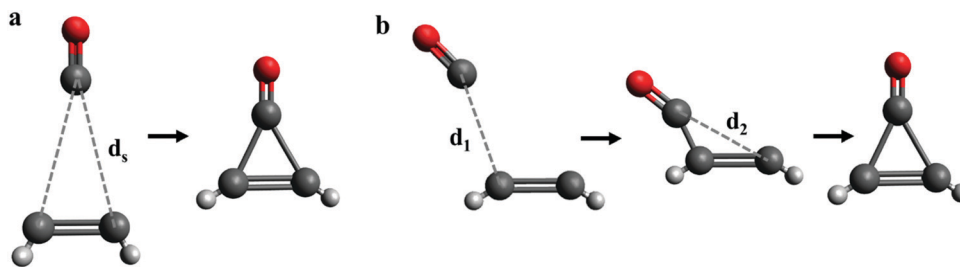


Fig. 4 Linear relationship of integrated ion counts of $m/z 58$ collected during the TPD phase of the $\text{C}^{18}\text{O}-\text{C}_2\text{D}_2$ ices photolyzed at 222 nm versus the photolysis time.

experiments at 288 nm (4.31 eV) excitation, only the lowest triplet state T1 is energetically accessible (*cis*- C_2H_2 ($a^3\text{B}_2$); *trans*- C_2H_2 ($a^3\text{B}_u$)); at 249 nm (4.98 eV), the second excited triplet state of acetylene T2 can be accessed (*cis*- C_2H_2 ($a^3\text{A}_2$); *trans*- C_2H_2 ($a^3\text{A}_u$)); as for the 222 nm (5.58 eV) excitation, the third excited triplet state T3 (*cis*- C_2H_2 ($b^3\text{B}_2$); *trans*- C_2H_2 ($b^3\text{B}_u$)) and the first excited singlet state S1 are energetically accessible (*cis*- C_2H_2 (A^1A_2); *trans*- C_2H_2 (A^1A_u)). Both concerted and stepwise mechanisms for the formation of cyclopropanone are explored (Scheme 4). The distances between the carbon atom of carbon monoxide and the carbon atoms of acetylene are labeled as d_s for the concerted mechanism and d_1/d_2 for the stepwise mechanism. The concerted mechanism maintains C_{2v} symmetry during the reaction and the stepwise mechanism has a reduced C_s symmetry. While the stepwise mechanism may also proceed without maintaining planar symmetry, CASPT2//CASSCF calculations indicated that the reactions have similar energetics when computed with or without enforcing C_s symmetry. Since the electronic states are easier to identify when symmetrized, C_s symmetry is used for all stepwise mechanism calculations.

Although an excitation to either the *cis* or the *trans* isomer for each excited state is energetically possible, the *trans* isomers cannot react in a concerted mechanism that maintains C_s symmetry. Furthermore, CASPT2//CASSCF calculations without symmetry constraints rule out a stepwise mechanism that involves a *trans* isomer, since a triplet intermediate, where bond d_1 is formed, was found to be unstable in the singlet ground state and undergoes barrierless dissociation to carbon monoxide and acetylene (Fig. S3, ESI†). Therefore, acetylene must be excited into a state in which the hydrogen atoms are oriented in a *cis* geometry. In the remainder of this section, using relaxed potential energy scans to simulate the concerted and stepwise mechanisms, we will discuss the reactivity of



Scheme 4 The proposed concerted (a, C_{2v} symmetry) and stepwise (b, C_s symmetry) mechanisms for the formation of $c\text{-C}_3\text{H}_2\text{O}$.

ground state carbon monoxide with excited states of *cis*-acetylene in its lowest three triplet (T1, T2, and T3) and the first singlet (S1) excited states.

2.3.1. Concerted reaction pathways. In all four excited low-lying *cis* states (T1, T2, T3, and S1), the excited state potential energy increases as carbon monoxide approaches perpendicularly to the acetylene carbon–carbon bond (Fig. 5). The concerted mechanism is not energetically feasible for the T2, T3 and S1 states (a^3A_2 , b^3B_2 , A^1A_2) under our experimental conditions since the energy along the reaction coordinate rises above 5.59 eV (222 nm) before crossing with a higher excited state of the same symmetry. The only state from which a concerted mechanism is energetically accessible is the T1 state (a^3B_2) since it comes close to the ground state before rising in energy. However, the formation of cyclopropenone from the

triplet excited state T1 (a^3B_2) requires intersystem crossing at a repulsive region of the T1 potential energy surface (PES). The spin–orbit coupling constant (SOCC) at the near-degeneracy at 2.2 \AA d_s is weak (1.79 cm^{-1} between the S_1 and $m_s = \pm 1$ components of T1), only increasing after leaving the near-degeneracy region of the PES (9.1 cm^{-1} at 1.8 \AA). Furthermore, the sloped topology of the T1 and ground state crossing region indicates that a concerted reaction is unlikely, and that intersystem crossing to the ground state would lead back to the unreacted reactants.

The results of the potential energy scans can be rationalized upon inspection of the orbital symmetries of the reactants and the cyclopropenone product (Fig. 6). The overall reaction involves a change of two electrons from A_1 to B_2 symmetry. While this could be achieved through an excited state with B_2

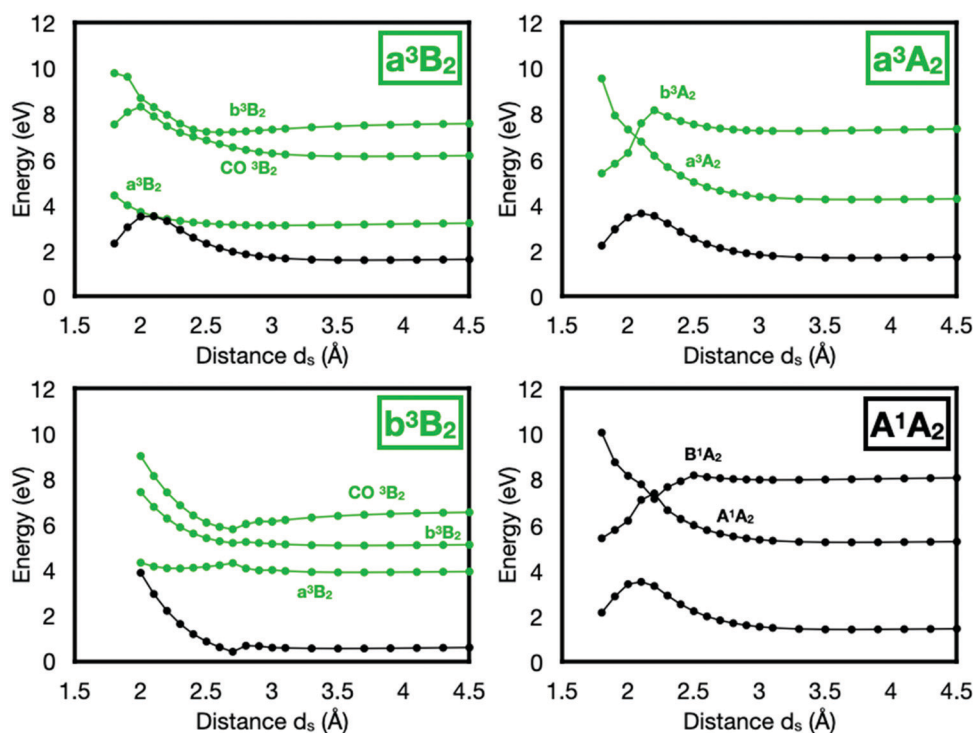


Fig. 5 Potential energy scans along d_s (Scheme 4) for the four lowest adiabatic excited states of acetylene (T1, T2, T3, and S1, corresponding to a^3B_2 , a^3A_2 , b^3B_2 , and A^1A_2). These calculations were carried out enforcing C_{2v} symmetry. The state for which gradients are used for the relaxed scan is indicated on the top right of each panel. Triplet states are indicated in green, while singlet states are indicated in black. The lowest singlet excited state in each panel is the ground state. Energies are reported relative to the ground state equilibrium geometry of acetylene and carbon monoxide at 4.5 \AA separation, *i.e.*, with linear acetylene.

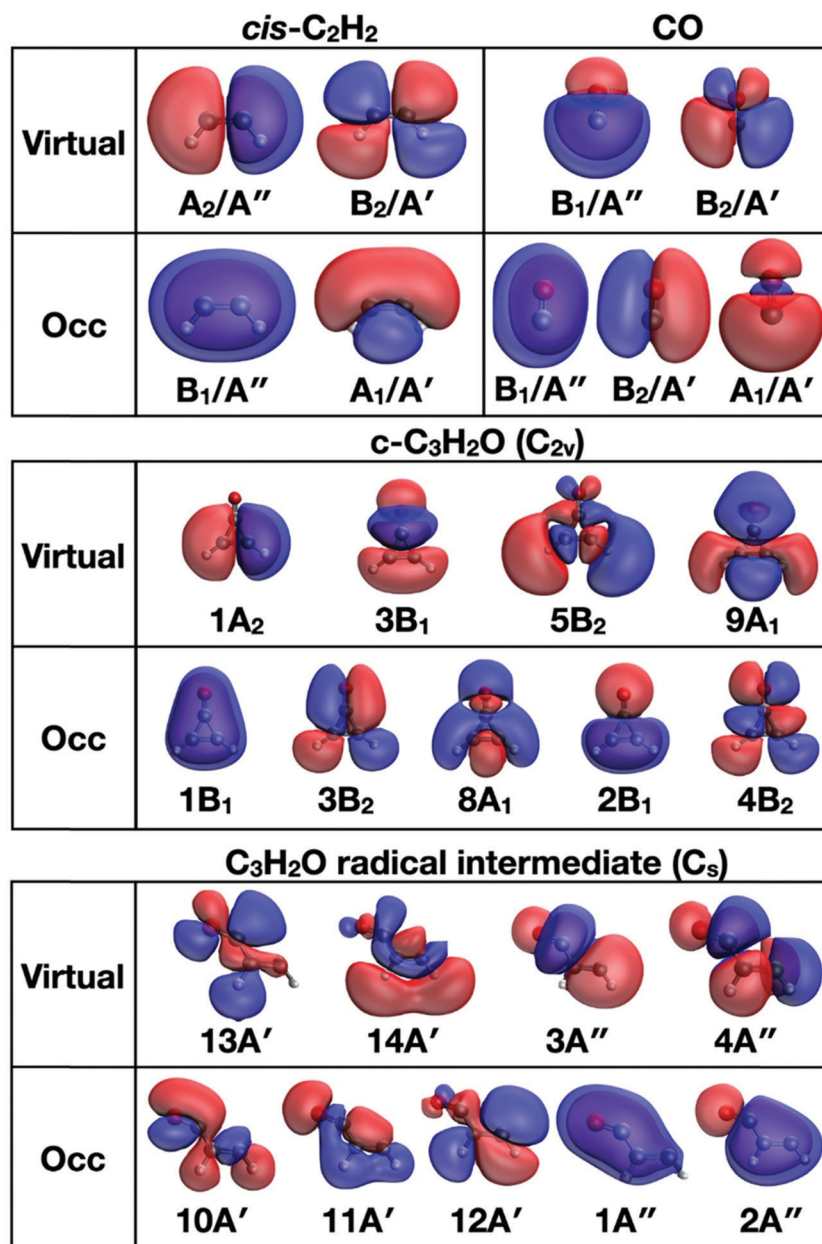


Fig. 6 Nine molecular orbitals used in the active space for CASPT2 and CASSCF calculations, shown for the reactants (top), product (middle), and open-shell intermediate (bottom). Specifically, the orbitals are shown for an excited-state optimized structure of acetylene in the *cis* stereoisomer, for carbon monoxide, and c-C₃H₂O (**3**) in their ground-state optimized structures, and a C₃H₂O radical optimized using the triplet state of the A' irreducible representation (a³A'). The molecular orbital labels use the C_{2v} irreducible representation for c-C₃H₂O (**3**), the C_s irreducible representation for the intermediate, and both C_s and C_{2v} irreducible representation for the reactants. Occ is an abbreviation for "occupied".

symmetry, one of the reactant A₁ orbitals becomes high in energy in the c-C₃H₂O product. A molecular orbital correlation would find that the reaction is effectively symmetry-forbidden when considering orbital reflection symmetry through the C_{2v} mirror planes.

2.3.2. Stepwise reaction pathways. The relaxed scans were repeated using C_s symmetry instead of C_{2v} such that only one distance, *d*₁, is constrained (Scheme 4). The potential energies along the relaxed scans for T1, T2, T3, and S1 (now labeled as

a³A', a³A'', b³A', and A¹A'' for C_s symmetry, and corresponding to a³B₂, a³A₂, b³B₂, and A¹A₂ for C_{2v} symmetry, respectively) are shown in Fig. 7. Except for T3 (b³A'), all states ultimately decrease in energy at small distances *d*₁ leading to an excited-state minimum that is (near)-degenerate with the ground state. In all cases, the excited-state minima have a structure where the carbon monoxide carbon is attached to one of the acetylene carbon atoms. This is in contrast to the concerted (C_{2v}) mechanism where these same states become unstable at short distances.

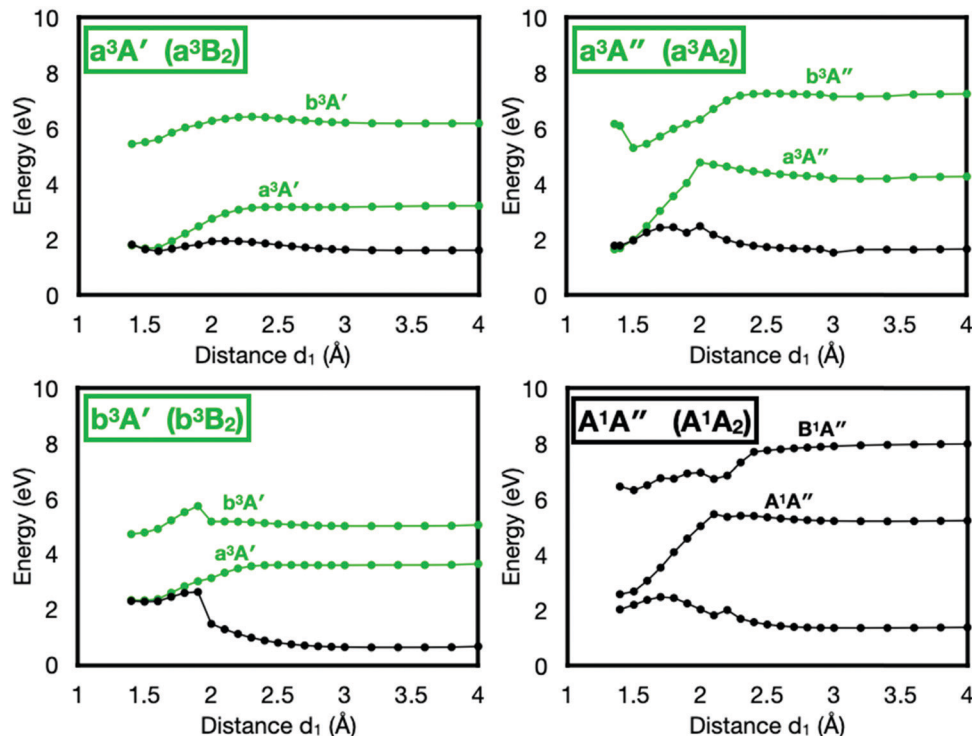


Fig. 7 Potential energy scans along d_1 (Scheme 4) for the four lowest adiabatic excited states of acetylene (T1, T2, T3, and S1, corresponding to a^3A' , a^3A'' , b^3A' , and A^1A''). These calculations were carried out enforcing C_s symmetry. The state for which gradients are used for the relaxed scan is indicated on the top right of each panel; both C_s and C_{2v} labels are used to help comparison with earlier figures. Triplet states are indicated in green, while singlet states are indicated in black. The lowest singlet excited state in each panel is the ground state. Energies are reported relative to the ground state equilibrium geometry of acetylene and carbon monoxide at 4.5 Å separation.

Overall, the potential energy scans suggest that the triplet states T1 and T2 (a^3A' and a^3A'') and singlet S1 (A^1A'') can decay through intersystem crossing or non-adiabatic coupling, respectively, to a ground state structure that already has one OC-C₂H₂ bond formed. On the other hand, the triplet state T3 (b^3A') would have to undergo internal conversion to the lower a^3A' triplet state before reaching the ground state. The computed spin orbit coupling (SOC) between the T2 (a^3A'') and singlet ground state at the T2 optimized geometry is 11.35 cm⁻¹. In contrast, the SOC between T1 (a^3A') and S0 does not exceed 2 cm⁻¹ in the near-degeneracy region. While there is no barrier for OC-C₂H₂ bond formation on the T1 state, the T2 and S1 states appear to have a barrier due to an avoided crossing with a higher excited state of the same symmetry prior to arriving at the excited-state minimum. Such a crossing must be energetically accessible at the photon energies used. The relaxed scans indicate a barrier on the order of 0.5 eV for the T2 (a^3A'') state and 0.2 eV for the S1 (A^1A'') state, but those are upper limits due to symmetry and geometry constraints used in the calculations.

If the low-lying T1 state forms an intermediate structure where a carbon-carbon single bond is formed between the carbon monoxide and acetylene, why is no product observed after experimentally exciting with 288 nm photons? Recall that cyclopropenone is only detected upon excitation with 249 nm and 222 nm photons, which means that the product can only be

formed from the T2 and S1 states corresponding to the a^3A_2 and A^1A_2 states under C_{2v} symmetry (Fig. S4, ESI†). To answer this question, we continue to map the reaction coordinate using a minimum energy path (MEP) calculation on the ground state PES starting from the T1 and T2 minimum-energy geometries (Fig. 8). Due to the close resemblance of the S1 and T2 minimum energy geometries, the MEP from the S1 is not included in the figure since it yields a similar energy profile as T2. An important difference between T1 and T2 is the geometry of the minimum-energy structure (the triplet intermediate). For T2 (a^3A'') as well as S1 (A^1A''), the C=O bond is collinear with the OC-C₂H₂ bond (Fig. 8 bottom). On the other hand, the T1 (a^3A') optimized structure has a carbon monoxide unit bonded at an OCC angle of 128°, parallel to the acetylene carbon-carbon bond (Fig. 8 top). These different structures reflect distinct electronic characters of both states. Running an MEP calculation starting from the T2 (a^3A'') and S1 (A^1A'') intermediate structures yields cyclopropenone (c-C₃H₂O, **3**) (Fig. 8 bottom). However, running an MEP starting from the T1 (a^3A') minimum structure quickly converges to an unstable intermediate with a similar structure having slightly modified bond lengths and OCC angle 126°. A relaxed scan on the ground state PES along an increasing d_1 bond length indicates that the dissociation of carbon monoxide from that intermediate is barrierless at the CASPT2//CASSCF level of theory (Fig. 8 top).

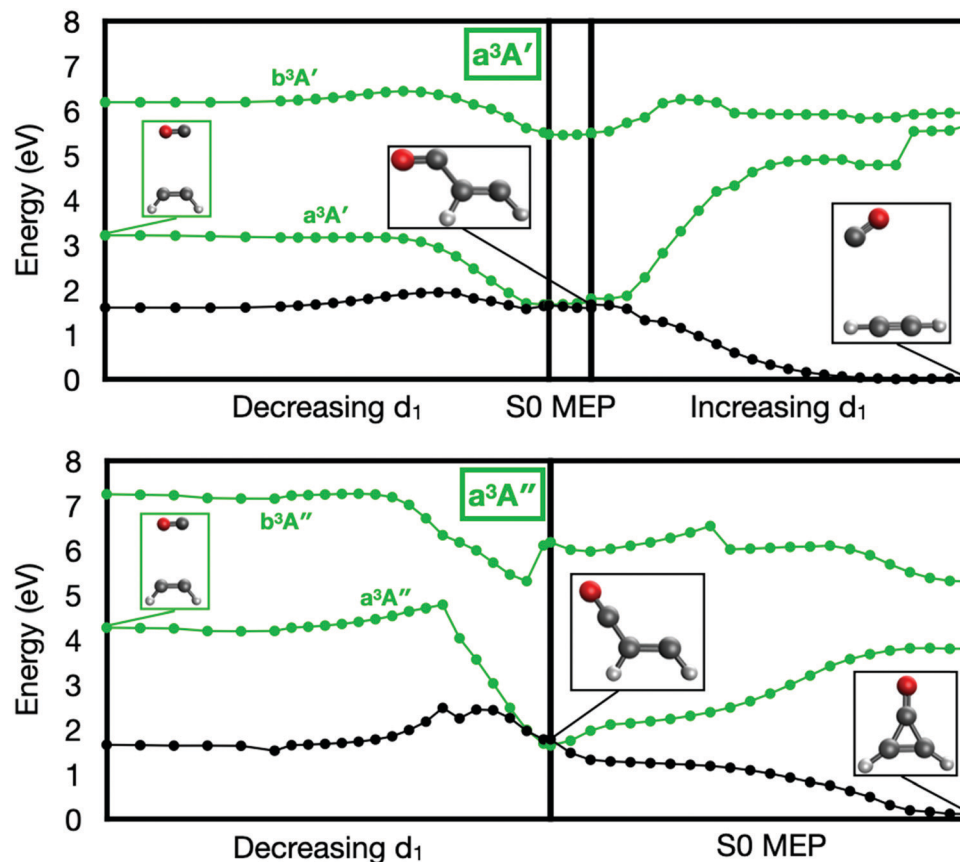


Fig. 8 Top: A combination of three calculations for the T1 state (a^3A'). The left plot is adapted from Fig. 5 and inverted to show decreasing rather than increasing d_1 . The central section is a minimum energy path (MEP) calculation on the ground state potential energy surface (PES), starting from the T1 (a^3A') triplet state minimum geometry. The plot on the right is a relaxed potential energy scan on the ground state PES while increasing the distance d_1 . Bottom: A combination of two calculations for the T2 (a^3A'') state. The left plot is adapted from Fig. 7 but inverted to show decreasing rather than increasing d_1 . The plot on the right is a MEP calculation on the ground state PES, starting from the triplet state T2 (a^3A'') minimum geometry. All calculations were carried out enforcing C_s symmetry. Triplet states are indicated in green, while singlet states are indicated in black. The lowest singlet excited state in each panel is the ground state. Energies are reported relative to the ground state equilibrium geometry of acetylene and carbon monoxide at 4.5 Å separation, *i.e.*, with a linear acetylene. Select structures for specific points are shown in boxes.

3. Conclusions

The joined experimental and computational investigation on the photolysis of acetylene-carbon monoxide ices provides persuasive testimony on stepwise cheletropic reaction pathways to cyclopropanone ($c\text{-C}_3\text{H}_2\text{O}$, **3**) *via* excited state dynamics involving the T2 (a^3A'') or S1 (A^1A'') states of acetylene. On the other hand, the reaction on the T1 (a^3A') state PES energetically favors an intermediate structure with a carbon-carbon single bond formed between carbon monoxide and acetylene that dissociates after relaxing to the ground state. The computational results agree well with the experiments, which reveal that cyclopropanone, as identified isomer-selectively *via* photoionization (PI) coupled with reflectron time-of-flight mass spectrometry (Re-TOF-MS), is only formed upon excitation of acetylene through a single-photon process with non-ionizing 222 nm and 249 nm photons, where S1 and T2 are energetically accessible, respectively, but not at 288 nm, where only T1 is energetically accessible. The overall reaction to yield $c\text{-C}_3\text{H}_2\text{O}$ from acetylene and carbon monoxide is endoergic by 57 kJ mol^{-1} , which can

be compensated by the excess energy of the photons. The strong agreement between the experiments in low temperature ices and the outcome of excited state calculations represents a key benchmark of how computational and experimental photochemistry can jointly be exploited as a tool to gain molecular-level insight into excited-state reaction mechanisms and untangle exotic non-equilibrium chemical processes.

The photochemistry leading to the formation of $c\text{-C}_3\text{H}_2\text{O}$ is not only interesting from the fundamental viewpoints of physical organic chemistry (*e.g.*, as unconventional non-equilibrium pathways to the formation of 2π - and 6π -aromatic ketones), but also reveals key insight into chemistry in more exotic environments such as ice-coated interstellar nanoparticles (interstellar grains) in cold molecular clouds and star-forming regions such as the Taurus Molecular Cloud (TMC-1) and Sagittarius-B2, (Sgr-B2), respectively.⁴⁷ Complex organic molecules (COMs) – organics containing more than six atoms of carbon, hydrogen, nitrogen, and oxygen such as aldehydes and ketones – are ubiquitous in the interstellar medium (ISM), but their formation mechanisms have remained largely obscure. While gas phase astrochemical reaction

networks replicate the abundance of hydrogen-deficient organics like linear cyanopolyynes,⁵⁸ pathways to complex organics are not understood. Since organic molecules constitute nearly 80% of all detected interstellar molecules, the untangling of the fundamental processes leading to these COMs is crucial to unravel the basic mechanisms that initiate and drive low temperature organic chemistry in space. Therefore, by exploiting cyclopropenone as a benchmark, laboratory astrophysics experiments coupled with theoretical calculations, as presented here, expose a hitherto overlooked reaction class leading to COMs *via* photon-triggered (non-adiabatic) excited state reactions. These processes may occur at ultralow temperatures (10 K) within interstellar ices, rather than through traditional radical–radical pathways on grain surfaces in the warm-up phase of the ices as hypothesized for the last decades, changing our perception on the formation of complex organics in the interstellar medium and eventually leading to the molecular precursors of biorelevant molecules as planets form in their interstellar nurseries.

4. Experimental and computational

4.1 Experimental section

The experiments were conducted in a contamination-free ultrahigh vacuum chamber pumped to a few 10^{-11} torr.⁴⁵ A 1 cm^2 silver mirror, which served as the substrate, was interfaced to a cold finger and cooled to $5.0 \pm 0.1\text{ K}$ by a closed-cycle helium compressor (Sumitomo Heavy Industries, RDK-415E). The $\text{C}^{18}\text{O}-\text{C}_2\text{D}_2$ ices were prepared by depositing gas mixtures of isotopically labeled ^{18}O -carbon monoxide (C^{18}O , 95% ^{18}O , Sigma Aldrich) and D_2 -acetylene (C_2D_2 , 99% D, CDN isotope) *via* a glass capillary array at a background pressure of 5×10^{-8} torr until ice thickness was achieved.⁵⁹ Since C_4H_6 isomers (54 amu) were detected in irradiated acetylene ices⁶⁰ and may overlap with cyclopropenone ($\text{C}_3\text{H}_2\text{O}$; 54 amu) formed by $\text{CO}-\text{C}_2\text{H}_2$ ices, isotopically labeled $\text{C}^{18}\text{O}-\text{C}_2\text{D}_2$ ices were used to be able to distinguish D_2-^{18}O cyclopropenone ($\text{C}_3\text{D}_2^{18}\text{O}$; 58 amu) and its isomers. An ice thickness of $960 \pm 30\text{ nm}$ was determined *in situ* using an estimated index of refraction of the mixed $\text{C}^{18}\text{O}-\text{C}_2\text{D}_2$ ice of 1.32 ± 0.03 . FTIR (Nicolet 6700) was used to monitor the $\text{C}^{18}\text{O}-\text{C}_2\text{D}_2$ ice mixture at 5 K both online and *in situ* before, during, and after the irradiation phase of the experiment in the range of 500 to 6000 cm^{-1} with a resolution of 4 cm^{-1} in intervals of approximately 2 minutes. After the deposition, the $\text{C}^{18}\text{O}-\text{C}_2\text{D}_2$ ice was photoexcited over a $1.0 \pm 0.1\text{ cm}^2$ area at an angle of incidence of 0° with respect to the surface normal of the substrate at wavelengths of 222 nm, 249 nm, and 288 nm with average laser powers of 10 mW. After the irradiation, the ice was sublimed *via* TPD as the substrate was heated to 300 K at 0.5 K min^{-1} . The analysis of any newly formed products in the gas phase after irradiation was achieved by the PI-ReTOF-MS.⁴⁶ More experimental details are included in the ESI.†

4.2 Computational section

To capture the multi-reference character of electronically excited acetylene during its reaction with CO, geometry optimizations

were carried out with the complete active space self-consistent field (CASSCF) method,⁵⁴ while single-point energy corrections are performed with the complete active space second-order perturbation theory (CASPT2) level of theory.⁵⁵ An active space of 10 electrons in 9 orbitals is employed for all calculations, shown in Fig. 6. In addition to symmetry constraints, relaxed scans were carried out by constraining the distance between the CO carbon atom and one of the C_2H_2 carbon atoms (d_s or d_1/d_2 in Scheme 4) at different values. Minimum energy path (MEP) calculations employed a step size of 0.05 bohr and a maximum step size of 0.02 bohr. All CASPT2 calculations employed an imaginary level shift of 0.2.⁶¹ No Ionization Potential-Electron Affinity (IPEA) shift was used.^{62,63} CASSCF geometry optimizations and CASPT2 energy and SOCC calculations were carried out using OpenMolcas version 21.06.⁶⁴ Natural transition orbitals (NTOs, Fig. S3, ESI†)^{65,66} for acetylene in the linear and bent (*cis* and *trans*) geometries were computed with time-dependent density functional theory using the B3LYP functional and 6-311++G** basis set. NTO calculations were performed with Q-Chem and visualized in IQmol.⁶⁷ Additional details of the computational methods are given in the ESI.†

Author contributions

The manuscript was written through the contributions of all authors. All authors have given approval to the final version of the manuscript.

Conflicts of interest

The authors declare no competing financial interest.

Acknowledgements

We thank the support of the US National Science Foundation (NSF) Division of Astronomical Sciences (AST) under Award NSF AST-2103269 to the University of Hawaii (R. I. K.). The experimental setup was financed by the W. M. Keck Foundation. Parts of the experiments and data analysis were supported by the Deutsche Forschungsgemeinschaft (DFG) through a Research Fellowship (KL 3342/1-1, N. F. K.). This material is in part based upon work supported by the National Science Foundation (NSF) under grant CHE-2047667 (S. G.). S. G. acknowledges NSF XSEDE for computational resources from Research Allocation CHE180027. We acknowledge the use of Advanced Research Computing Technology and Innovation Core (ARCTIC) resources at Georgia State University's Research Solutions, made available by the National Science Foundation Major Research Instrumentation (MRI) grant number CNS-1920024.

References

- 1 A. Kilaj, J. Wang, P. Stranak, M. Schwillk, U. Rivero, L. Xu, O. A. von Lilienfeld, J. Kupper and S. Willitsch, Conformer-specific

- polar cycloaddition of dibromobutadiene with trapped propene ions, *Nat. Commun.*, 2021, **12**(1), 6047.
- 2 E. M. Greer and C. V. Cosgriff, Reaction mechanisms: pericyclic reactions, *Annu. Rep. Prog. Chem., Sect. B: Org. Chem.*, 2013, **109**(0), 328–350.
 - 3 B. K. Decker, L. M. Babcock and N. G. Adams, Selected Ion Flow Tube Studies of S + (4S) Reactions with Small Oxygenated and Sulfurated Organic Molecules, *J. Phys. Chem. A*, 2000, **104**(4), 801–810.
 - 4 R. B. Woodward and R. Hoffmann, The Conservation of Orbital Symmetry, *Angew. Chem., Int. Ed. Engl.*, 1969, **8**(11), 781–853.
 - 5 R. B. Woodward and R. Hoffmann, Stereochemistry of Electrocyclic Reactions, *J. Am. Chem. Soc.*, 1965, **87**(2), 395–397.
 - 6 Y. Liu, K. Bakshi, P. Zavalij and M. P. Doyle, Pericyclic Reaction of a Zwitterionic Salt of an Enedione-diazoester. A Novel Strategy for the Synthesis of Highly Functionalized Resorcinols, *Org. Lett.*, 2010, **12**(19), 4304–4307.
 - 7 H. Vančik, *Pericyclic Reactions. In Basic Organic Chemistry for the Life Sciences*, Springer, 2022, pp. 137–140.
 - 8 K. Fukui, T. Yonezawa and H. Shingu, A Molecular Orbital Theory of Reactivity in Aromatic Hydrocarbons, *J. Chem. Phys.*, 1952, **20**(4), 722–725.
 - 9 H. Longuet-Higgins and E. Abrahamson, The electronic mechanism of electrocyclic reactions, *J. Am. Chem. Soc.*, 1965, **87**(9), 2045–2046.
 - 10 F. Bernardi, P. Celani, M. Olivucci, M. A. Robb and G. Suzzivalli, Theoretical Study of the Aromatic Character of the Transition States of Allowed and Forbidden Cycloadditions, *J. Am. Chem. Soc.*, 1995, **117**(42), 10531–10536.
 - 11 P. B. Karadakov, J. Gerratt, D. L. Cooper and M. Raimondi, Spin-coupled description of organic reaction pathways: the cycloaddition reaction of two ethene molecules, *J. Chem. Soc., Faraday Trans.*, 1994, **90**(12), 1643–1651.
 - 12 D. Y. Kim, D. C. Yang, J. M. L. Madrideojos, A. Hajibabaei, C. Baig and K. S. Kim, Anisotropic and amphoteric characteristics of diverse carbenes, *Phys. Chem. Chem. Phys.*, 2018, **20**(20), 13722–13733.
 - 13 M. Sironi, M. Raimondi, D. L. Cooper and J. Gerratt, The electronic structure of CH₂ and the cycloaddition reaction of methylene with ethene, *J. Chem. Soc., Faraday Trans. 2*, 1987, **83**(9), 1651–1661.
 - 14 J. A. Miller and C. F. Melius, Kinetic and thermodynamic issues in the formation of aromatic compounds in flames of aliphatic fuels, *Combust. Flame*, 1992, **91**(1), 21–39.
 - 15 D. Polino, S. J. Klippenstein, L. B. Harding and Y. Georgievskii, Predictive Theory for the Addition and Insertion Kinetics of 1CH₂ Reacting with Unsaturated Hydrocarbons, *J. Phys. Chem. A*, 2013, **117**(48), 12677–12692.
 - 16 W. Mahler, Double Addition of a Carbene to an Acetylene, *J. Am. Chem. Soc.*, 1962, **84**(23), 4600–4601.
 - 17 L. Ye, Y. Georgievskii and S. J. Klippenstein, Pressure-dependent branching in the reaction of 1CH₂ with C₂H₄ and other reactions on the C₃H₆ potential energy surface, *Proc. Combust. Inst.*, 2015, **35**(1), 223–230.
 - 18 W. v E. Doering and T. Mole, Stereo-selectivity in the reaction of carbomethoxycarbene with *cis*-butene, *Tetrahedron*, 1960, **10**(1), 65–70.
 - 19 R. Neidlein, M. Kohl and W. Kramer, Herstellung substituerter 1,6-Methano[10]annulene durch Cycloadditionsreaktionen des 1H-Cyclopropabenzols, *Helv. Chim. Acta*, 1989, **72**(6), 1311–1318.
 - 20 J.-M. Brunel, R. Villard and G. Buono, Synthesis of new chiral σ 2 λ 2-phosphenium cations, *Tetrahedron Lett.*, 1999, **40**(25), 4669–4672.
 - 21 K. C. Nicolaou, G. Vassilikogiannakis, W. Mägerlein and R. Kranich, Total Synthesis of Colombiasin A, *Angew. Chem., Int. Ed.*, 2001, **40**(13), 2482–2486.
 - 22 K. C. Nicolaou, G. Zuccarello, C. Riemer, V. A. Estevez and W. M. Dai, Design, synthesis, and study of simple monocyclic conjugated enediyne. The 10-membered ring enediyne moiety of the enediyne anticancer antibiotics, *J. Am. Chem. Soc.*, 1992, **114**(19), 7360–7371.
 - 23 G. B. Gill and M. R. Willis, *The stereochemical requirements of concentrated pericyclic reactions. In Pericyclic Reactions*, Springer Netherlands, Dordrecht, 1974, pp. 63–98.
 - 24 A. G. Anastassiou and H. Yamamoto, Thermal cheletropy in model azabicycles; the question of linear vs. non-linear extrusion, *J. Chem. Soc., Chem. Commun.*, 1973, (21), 840–841.
 - 25 A. Arrieta, A. de Cozar and F. P. Cossio, Cyclic Electron Delocalization in Pericyclic Reactions, *Curr. Org. Chem.*, 2011, **15**(20), 3594–3608.
 - 26 M. Rosenberg, C. Dahlstrand, K. Kilså and H. Ottosson, Excited State Aromaticity and Antiaromaticity: Opportunities for Photophysical and Photochemical Rationalizations, *Chem. Rev.*, 2014, **114**(10), 5379–5425.
 - 27 K. H. R. Hennigar and R. F. Langler, An Alternative Platform for the Assessment of Hckel and Mbius Transition States in Concerted Reactions, *Aust. J. Chem.*, 2010, **63**(3), 490–501.
 - 28 A. G. Middleton, M. J. Brunger and P. J. O. Teubner, Excitation of the electronic states of carbon monoxide by electron impact, *J. Phys. B: At., Mol. Opt. Phys.*, 1993, **26**(11), 1743–1759.
 - 29 S. W. S. Wilson, C. L. Reed, D. H. Mordaunt, M. Ashfold and M. Kawasaki, Near-Threshold Photodissociation of C₂H₂, C₂HD, and C₂D₂ Studied by H(D) Atom Photofragment Translational Spectroscopy, *Bull. Chem. Soc. Jpn.*, 1996, **69**(1), 71–76.
 - 30 P. Erman, A. Karawajczyk, E. Rachlew-Källne, C. Strömholm, J. Larsson, A. Persson and R. Zerne, Direct determination of the ionization potential of CO by resonantly enhanced multiphoton ionization mass spectroscopy, *Chem. Phys. Lett.*, 1993, **215**(1), 173–178.
 - 31 R. H. Schuler and F. A. Stuber, Comparative Ionization by Million-Electron-Volt Heavy Ions and Kilolectron-Volt Electrons, *J. Chem. Phys.*, 1964, **40**(7), 2035–2036.
 - 32 R. C. Benson, W. H. Flygare, M. Oda and R. Breslow, Microwave spectrum, substitutional structure, and Stark and Zeeman effects in cyclopropanone, *J. Am. Chem. Soc.*, 1973, **95**(9), 2772–2777.

- 33 W. R. Harshbarger, N. A. Kuebler and M. B. Robin, Electronic structure and spectra of small rings. V Photoelectron and electron impact spectra of cyclopropenone, *J. Chem. Phys.*, 1974, **60**(2), 345–350.
- 34 C. A. Jacobs, J. C. Brahms, W. P. Dailey, K. Beran and M. D. Harmony, Synthesis, microwave spectrum, and ab initio calculations for difluorocyclopropenone, *J. Am. Chem. Soc.*, 1992, **114**(1), 115–121.
- 35 H. Wang and K. Brezinsky, Computational Study on the Thermochemistry of Cyclopentadiene Derivatives and Kinetics of Cyclopentadienone Thermal Decomposition, *J. Phys. Chem. A*, 1998, **102**(9), 1530–1541.
- 36 U. Eckart, M. P. Fülcher, L. Serrano-Andrés and A. J. Sadlej, Static electric properties of conjugated cyclic ketones and thioketones, *J. Chem. Phys.*, 2000, **113**(15), 6235–6244.
- 37 L. Serrano-Andrés, R. Pou-Amérigo, M. P. Fülcher and A. C. Borin, Electronic excited states of conjugated cyclic ketones and thioketones: A theoretical study, *J. Chem. Phys.*, 2002, **117**(4), 1649–1659.
- 38 K. Najafian, P. von Ragué Schleyer and T. T. Tidwell, Aromaticity and antiaromaticity in fulvenes, ketocyclopolyenes, fulvenones, and diazocyclopolyenes, *Org. Biomol. Chem.*, 2003, **1**(19), 3410–3417.
- 39 H. R. Paudel, L. J. Karas and J. I. C. Wu, On the reciprocal relationship between σ -hole bonding and (anti)aromaticity gain in ketocyclopolyenes, *Org. Biomol. Chem.*, 2020, **18**(27), 5125–5129.
- 40 A. Yusufjiang and A. Kerim, A study on the aromaticity and ring currents of polycyclic neutral oxocarbon isomers, *J. Phys. Org. Chem.*, 2021, **34**(12), e4271.
- 41 C. Liu, Y. Ni, X. Lu, G. Li and J. Wu, Global Aromaticity in Macrocyclic Polyradicaloids: Hückel's Rule or Baird's Rule?, *Acc. Chem. Res.*, 2019, **52**(8), 2309–2321.
- 42 P. A. Peart and J. D. Tovar, Poly(cyclopropenone)s: Formal Inclusion of the Smallest Hückel Aromatic into π -Conjugated Polymers, *J. Org. Chem.*, 2010, **75**(16), 5689–5696.
- 43 G. L. Bottger and D. F. Eggers Jr., Infrared Spectra of Crystalline C₂H₂, C₂H₂D, and C₂D₂, *J. Chem. Phys.*, 1964, **40**(7), 2010–2017.
- 44 C. S. Jamieson, A. M. Mebel and R. I. Kaiser, Understanding the Kinetics and Dynamics of Radiation-induced Reaction Pathways in Carbon Monoxide Ice at 10 K, *Astrophys. J., Suppl. Ser.*, 2006, **163**(1), 184–206.
- 45 R. I. Kaiser, S. Maity and B. M. Jones, Infrared and reflectron time-of-flight mass spectroscopic analysis of methane (CH₄)-carbon monoxide (CO) ices exposed to ionization radiation – toward the formation of carbonyl-bearing molecules in extraterrestrial ices, *Phys. Chem. Chem. Phys.*, 2014, **16**(8), 3399–3424.
- 46 M. J. Abplanalp, M. Förstel and R. I. Kaiser, Exploiting single photon vacuum ultraviolet photoionization to unravel the synthesis of complex organic molecules in interstellar ices, *Chem. Phys. Lett.*, 2016, **644**, 79–98.
- 47 A. M. Turner and R. I. Kaiser, Exploiting Photoionization Reflectron Time-of-Flight Mass Spectrometry to Explore Molecular Mass Growth Processes to Complex Organic Molecules in Interstellar and Solar System Ice Analogs, *Acc. Chem. Res.*, 2020, **53**(12), 2791–2805.
- 48 M. J. Abplanalp, A. Borsuk, B. M. Jones and R. I. Kaiser, On the formation and isomer specific detection of propenal (C₂H₃CHO) and cyclopropanone (c-C₃H₄O) in interstellar model ices—a combined FTIR and reflectron time-of-flight mass spectroscopic study, *Astrophys. J.*, 2015, **814**(1), 45.
- 49 O. Kostko, B. Bandyopadhyay and M. Ahmed, Vacuum Ultraviolet Photoionization of Complex Chemical Systems, *Annu. Rev. Phys. Chem.*, 2016, **67**(1), 19–40.
- 50 W. von Niessen, G. Bieri and L. Åsbrink, 30.4-nm He (II) photoelectron spectra of organic molecules: Part III. Oxocompounds (C, H, O), *J. Electron Spectrosc. Relat. Phenom.*, 1980, **21**(2), 175–191.
- 51 J. K. Terlouw, J. L. Holmes and F. P. Lossing, Ionized ethylidene ketene and its homologue methylene ketene, *Can. J. Chem.*, 1983, **61**(8), 1722–1724.
- 52 N. F. Kleimeier, M. J. Abplanalp, R. N. Johnson, S. Gozem, J. Wandishin, C. N. Shingledecker and R. I. Kaiser, Cyclopropenone (c-C₃H₂O) as a Tracer of the Nonequilibrium Chemistry Mediated by Galactic Cosmic Rays in Interstellar Ices, *Astrophys. J.*, 2021, **911**(1), 24.
- 53 M. J. Abplanalp and R. I. Kaiser, On the formation of complex organic molecules in the interstellar medium: untangling the chemical complexity of carbon monoxide-hydrocarbon containing ice analogues exposed to ionizing radiation via a combined infrared and reflectron time-of-flight analysis, *Phys. Chem. Chem. Phys.*, 2019, **21**(31), 16949–16980.
- 54 B. O. Roos, P. R. Taylor and P. E. M. Sigbahn, A complete active space SCF method (CASSCF) using a density matrix formulated super-CI approach, *Chem. Phys.*, 1980, **48**(2), 157–173.
- 55 K. Andersson, P.-Å. Malmqvist, B. Roos, A. J. Sadlej and K. Wolinski, Second-order perturbation theory with a CASSCF reference function, *J. Phys. Chem.*, 1990, **94**, 5483–5488.
- 56 J. Almlöf and P. R. Taylor, General contraction of Gaussian basis sets. I. Atomic natural orbitals for first- and second-row atoms, *J. Chem. Phys.*, 1987, **86**(7), 4070–4077.
- 57 P.-O. Widmark, P.-Å. Malmqvist and B. O. Roos, Density matrix averaged atomic natural orbital (ANO) basis sets for correlated molecular wave functions, *Theor. Chim. Acta*, 1990, **77**(5), 291–306.
- 58 R. I. Kaiser and N. Balucani, Exploring the Gas Phase Synthesis of the Elusive Class of Boronyls and the Mechanism of Boronyl Radical Reactions under Single Collision Conditions, *Acc. Chem. Res.*, 2017, **50**(5), 1154–1162.
- 59 S. Maity, R. I. Kaiser and B. M. Jones, Formation of ketene (H₂CCO) in interstellar analogous methane (CH₄)-carbon monoxide (CO) ices: A combined FTIR and reflectron time-of-flight mass spectroscopic study, *Astrophys. J.*, 2014, **789**(1), 36.
- 60 M. J. Abplanalp and R. I. Kaiser, Implications for Extraterrestrial Hydrocarbon Chemistry: Analysis of Acetylene (C₂H₂) and D₂-acetylene (C₂D₂) Ices Exposed to Ionizing Radiation via Ultraviolet-Visible Spectroscopy, Infrared

- Spectroscopy, and Reflectron Time-of-flight Mass Spectrometry, *Astrophys. J.*, 2020, **889**(1), 3.
- 61 N. Forsberg and P.-Å. Malmqvist, Multiconfiguration perturbation theory with imaginary level shift, *Chem. Phys. Lett.*, 1997, **274**(1), 196–204.
- 62 J. P. Zobel, J. J. Nogueira and L. González, The IPEA dilemma in CASPT2, *Chem. Sci.*, 2017, **8**(2), 1482–1499.
- 63 G. Ghigo, B. O. Roos and P.-Å. Malmqvist, A modified definition of the zeroth-order Hamiltonian in multiconfigurational perturbation theory (CASPT2), *Chem. Phys. Lett.*, 2004, **396**(1), 142–149.
- 64 I. Fdez Galván, M. Vacher, A. Alavi, C. Angeli, F. Aquilante, J. Autschbach, J. J. Bao, S. I. Bokarev, N. A. Bogdanov and R. K. Carlson, OpenMolcas: From Source Code to Insight, *J. Chem. Theory Comput.*, 2019, **15**(11), 5925–5964.
- 65 M. Head-Gordon, A. M. Grana, D. Maurice and C. A. White, Analysis of Electronic Transitions as the Difference of Electron Attachment and Detachment Densities, *J. Phys. Chem.*, 1995, **99**(39), 14261–14270.
- 66 R. L. Martin, Natural transition orbitals, *J. Chem. Phys.*, 2003, **118**(11), 4775–4777.
- 67 E. Epifanovsky, A. T. B. Gilbert, X. Feng, J. Lee, Y. Mao, N. Mardirossian, P. Pokhilko, A. F. White, M. P. Coons and A. L. Dempwolff, Software for the frontiers of quantum chemistry: An overview of developments in the Q-Chem 5 package, *J. Chem. Phys.*, 2021, **155**(8), 084801.